Pergamon

Geochimica et Cosmochimica Acta, Vol. 67, No. 23, pp. 4639–4654, 2003

0016-7037/03 $30.00 + .00

doi:10.1016/S0016-7037(03)00389-2

Stable isotope compositions of cadmium in geological materials and meteorites determined by multiple-collector ICPMS

FRANK WOMBACHER,[1,*] MARK REHKÄMPER,[2] KLAUS MEZGER,[1] and CARSTEN MÜNKER[1]

[1]Institut für Mineralogie, Universität Münster, Corrensstr. 24, 48149 Münster, Germany
[2]Institut für Isotopengeologie und Mineralische Rohstoffe, ETH Zürich, NO C61, CH-8092 Zürich, Switzerland

(*Received November* 25, 2002; *accepted in revised form May* 30, 2003)

Abstract—A new technique for the precise and accurate determination of Cd stable isotope compositions has been developed and applied to geological materials and meteorites. The Cd isotope analyses are performed by multiple collector inductively coupled plasma mass spectrometry (MC-ICPMS) using external normalization to Ag for mass bias correction. The accuracy of the new procedure was ascertained by the comparison of data for meteorites with published results acquired by thermal ionization mass spectrometry and double spiking. Some results were also confirmed by measurements using external normalization to Sb on a different MC-ICPMS instrument. A long-term reproducibility of ± 1.1 εCd/amu (2 sd) was obtained for separate dissolutions and multiple analyses of several rock and meteorite samples (εCd/amu represents the deviation of a Cd isotope ratio of a sample relative to the JMC Cd standard in parts per 10^4, normalized to a mass difference of 1 amu). As little as 5–20 ng of Cd are sufficient for the acquisition of precise and accurate data.

Terrestrial rock and mineral samples display little variations in Cd isotope compositions (εCd/amu between −1 and +1.2), except for a tektite sample that was found to be enriched in the heavy Cd isotopes by +7.6 εCd/amu. The carbonaceous chondrites Orgueil, Murchison and Allende have Cd isotope ratios that are unfractionated relative to the JMC Cd standard and terrestrial rocks. The ordinary chondrites analyzed in this study and a Rumuruti chondrite display Cd isotope fractionations, ranging from −19 to +36 εCd/amu.

These results suggest that substantial (inorganic) natural Cd isotope fractionations are generated only by evaporation and/or condensation processes. The lack of resolvable Cd isotope variations between the different carbonaceous chondrites, despite large differences in Cd concentrations, implies that the primary depletion of Cd in the early solar system did not involve Rayleigh evaporation. The Cd isotope fractionation in ordinary and Rumuruti chondrites is probably due to the redistribution of Cd by evaporation and condensation processes during thermal metamorphism on the parent bodies. Models that explain the enrichments of highly volatile elements in unequilibrated ordinary chondrites by primary equilibrium condensation appear to be inconsistent with the Cd isotope data.

1. INTRODUCTION

Cadmium is a trace element which occurs at ppb level abundances in rocks and meteorites. It has eight stable isotopes that span 10 atomic mass units (amu) with a relative mass difference of 9.4% (Table 1). In nature, Cd occurs as a divalent cation that forms bonds of predominantly ionic character. Therefore, Cd stable isotope fractionations due to geological processes are expected to be small. In an early study, Rosman and De Laeter (1975) reported that Cd isotope fractionations in terrestrial minerals do not exceed 1‰ per atomic mass unit. In cosmochemistry, Cd is classified as a highly volatile element with a 50% condensation temperature T_C = 430 K at 10^{-5} bar (=1 Pa) (Larimer, 1973). Several studies identified large mass-dependent Cd isotope fractionations in chondritic meteorites and lunar soils that range from −21 to +63 εCd/amu (Rosman and De Laeter, 1976; Rosman and De Laeter, 1978; Rosman et al., 1980a,b; Rosman and De Laeter, 1988; Sands et al., 2001). It has been suggested that the Cd isotope fractionations in chondritic meteorites result from Rayleigh distillation, primordial heterogeneities or nebular processes (Rosman and De Laeter, 1978; Rosman et al., 1980b; Rosman and De Laeter, 1988).

Previous Cd isotope studies were carried out by thermal ionization mass spectrometry (TIMS), generally in conjunction with double spiking for the precise correction of instrumental mass discrimination (Rosman and De Laeter, 1976; Rosman et al., 1980a,b; Rosman and De Laeter, 1988). Such measurements, however, are rendered difficult by the high first ionization potential of Cd and the analytical uncertainties that were reported range from ±0.6 to ±10 εCd/amu for single sample measurements.

Plasma source mass spectrometers readily overcome the problem of the low ionization efficiency of Cd in the TIMS source and are suitable for high precision isotope ratio measurements if they are equipped with an array of Faraday cup detectors. Such multiple collector inductively coupled plasma mass spectrometers (MC-ICPMS) display an instrumental mass discrimination that is far more pronounced than in TIMS. However, the severe mass discrimination (~2% per amu mass difference for Cd) can be controlled with a number of different analytical strategies (Longerich et al., 1987; Walder and Furuta, 1993; Hirata, 1997; Belshaw et al., 1998; Maréchal et al., 1999; Tomascak et al., 1999; Siebert et al., 2001). As a consequence, MC-ICPMS analyses have spurred investigations of mass-dependent isotope fractionations even for "heavy" elements with atomic masses > 40 amu (e.g., Rehkämper et al., in press).

Here we present a MC-ICPMS technique for the precise and

* Author to whom correspondence should be addressed, at GEOMAR Forschungszentrum für Marine Geowissenschaften, Wischofstr. 1-3, 24148, Kiel, Germany (fwombacher@geomar.de).

Table 1. Collector configurations, isotope abundances and major interferences.

Mass	106	107	108	109	110	111	112	113	114	115	116	117	118	120	121	123
Collector configuration																
Nu main run	L5	L4	L3	L2	Ax	H2	H4	H5	H6							
Nu interf. run						L4	L3	L2	Ax	H2	H4	H5	H6			
IsoP. Ag-Cd	L3	L2		Ax	H1	H2	H3		H4		H5	H6				
IsoP. Sb-Cd					L3			L2	Ax	H1	H2	H3		H4	H5	H6
Isotope abundances (%)																
Pd	27.3		26.5		11.7											
Ag		51.8		48.2												
Cd	1.25		0.89		12.5	12.8	24.1	12.2	28.7		7.49					
In								4.3		95.7						
Sn							0.97		0.65	0.36	14.5	7.68	24.2	32.6		
Sb															57.3	42.7
Major molecular interferences and isotope abundances (%)																
$M^{40}Ar^+$	^{66}Zn	^{67}Zn	^{68}Zn	^{69}Ga	^{70}Ge	^{71}Ga	^{72}Ge	^{73}Ge	^{74}Ge	^{75}As	^{76}Ge	^{77}Se	^{78}Se	^{80}Se	^{81}Br	^{83}Kr
	27.9	*4.1*	*18.8*	*60.1*	*20.5*	*39.9*	*27.4*	*7.8*	*36.5*	*100*	*7.8*	*7.6*	*23.6*	*49.7*	*49.3*	*11.5*
					^{70}Zn						^{76}Se		^{78}Kr	^{80}Kr		
					0.6						9.0		*0.35*	*2.25*		
$M^{16}O^+$	^{90}Zr	^{91}Zr	^{92}Zr	^{93}Nb	^{94}Zr	^{95}Mo	^{96}Zr	^{97}Mo	^{98}Mo	^{99}Ru	^{100}Mo	^{101}Ru	^{102}Ru	^{104}Ru	^{105}Pd	^{107}Ag
	51.5	*11.2*	*17.2*	*100*	*17.4*	*15.9*	*2.80*	*9.55*	*24.1*	*12.7*	*9.63*	17.0	31.6	*18.7*	*22.3*	*51.8*
			^{92}Mo		^{94}Mo		^{96}Mo		^{98}Ru		^{100}Ru		^{102}Pd	^{104}Pd		
			14.8		*9.25*		*16.7*		*1.88*		*12.6*		1.02	*11.1*		
							^{96}Ru									
							5.52									

accurate determination of Cd isotope compositions in geological samples and meteorites. Separation of Cd from such samples is performed using a improved two-stage column chemistry procedure. Furthermore, we investigate the advantages and disadvantages of different mass bias correction procedures. With the new techniques, Cd stable isotope compositions can be accurately determined from only 5 ng of sample Cd and with a precision that is superior to most published double spike-TIMS data. Samples selected for this study include Cd (-rich) minerals, an experimentally precipitated aragonite, sedimentary, igneous and impact-related terrestrial rocks and chondritic meteorites.

2. EXPERIMENTAL PROCEDURES

2.1. Sample Preparation

2.1.1. Reagents and Materials

All acids used in this study were purified by subboiling distillation and the water was 18 MΩ grade from a Millipore system. The HNO_3-HBr mixtures that are required for the anion-exchange chemistry were prepared freshly on the day of use, because both acids slowly react with one another.

A 1000 μg/mL JMC Cd solution (Johnson Matthey Co. ICP standard Lot: 502552A, supplied by Alfa Aesar, Germany), and dilute solutions prepared from this, was used as Cd isotope reference standard. A solution of VTA-3 Cd in dilute HNO_3 served as a secondary (fractionated) Cd isotope standard. The VTA-3 Cd was prepared at Vacuum Technology Aalen, Germany by the evaporation of Cd in a vacuum chamber and recondensation of the vapor onto a glass slide.

2.1.2. Sample Digestion

For rock and meteorite samples, typically 100 to 500 mg of powder were weighed into 15 mL Savillex beakers. Two grams of rock powder were used for a layered tektite sample and between 0.9 and 3.2 g for most impact melt coated gneiss bomb samples.

About 3 mL of 14.3 mol/L HNO_3 were added to the rock powders, the beakers capped and the samples oxidized on a hot plate and subsequently dried down. About 1 mL of both 14.3 mol/L HNO_3 and 28 mol/L HF were added/100 mg of rock powder, and the samples were digested in an oven at 200°C for at least 30 h with the Savillex beakers placed inside Teflon-sealed Parr bombs. After drying, the samples were repeatedly refluxed with acid for several hours in capped beakers at 160°C on a hot plate, first three times with 14.3 mol/L HNO_3, then three times with 6 mol/L HCl. The final 6 mol/L HCl solutions were diluted with 0.5 mol/L HCl to obtain 3 M HCl. This procedure resulted in clear solutions for most samples. Gels or white precipitates that formed in some cases were separated by centrifugation. If significant coprecipitation of Cd were to occur at this stage, this could result in solutions that have fractionated Cd isotope compositions. However, no systematic relationship between the occurrence of precipitates and the Cd isotope composition was found for multiple dissolutions of several geological samples and this indicates that the data are not significantly affected by such fractionation effects.

2.1.3. Chemical Separation

To avoid interferences and matrix effects, chemical separation of Cd from the sample matrix is a prerequisite for precise isotope ratio measurements. Separation of Cd from the elements Pd, In, and Sn is particularly important, because these elements can generate direct isobaric interferences (Table 1). As discussed below, a Ag standard was added to the sample and standard solutions for external mass bias correction during measurements. This correction requires that both sample and standard solutions contain Ag with the same isotope composi-

Table 2. Elution sequence of the anion-exchange and the TRU Spec resin chemistry for the separation of Cd.

Eluent	Volume (ml)	Eluted
2 mL Biorad AG 1-X8 anion-exchange resin (100–200 mesh)[a]		
2 M HNO_3 (resin cleaning)	10	
8 M HCI (wash, conversion to Cl^- form)	20	
0.5 M HCl (wash, conversion to Cl^- form)	10	
3 M HCl (resin conditioning)	10	
3 M HCl (sample solution)	10–12	matrix
0.5 M HCl	30	matrix
1 M HCl	10	matrix
2 M HCl	10	matrix
8 M HCl	12	Ag
0.5 M HNO_3-0.1 M HBr	2.5	
0.5 M HNO_3-0.1 M HBr	10	Zn
2 M HNO_3	2.5	
2 M HNO_3	8	Cd
120 μL Eichrom TRU Spec resin[b]		
6 M HCl (resin conditioning)	10	
8 M HCl (sample solution)	0.2	Cd
8 M HCl (rinse of sample beaker)	0.2	Cd
6 M HCl	1.4	Cd

[a] Columns are made of shrinkable Kynar tubes. The resin bed is 5.5 mm in diameter and 85 mm high. The resin is not reused.

[b] Columns are made of shrinkable Teflon. The resin bed has a diameter of 2.2 mm. The resin is not reused.

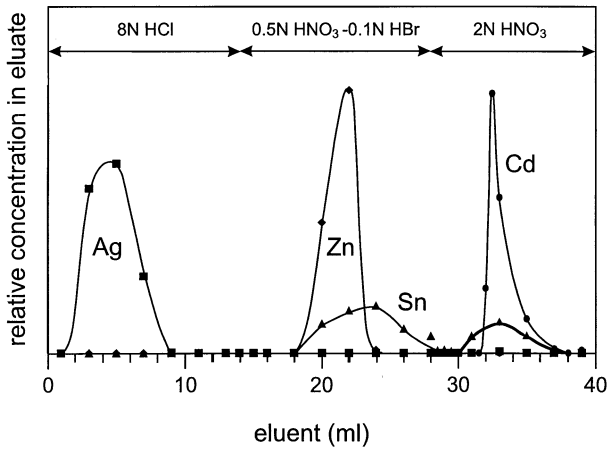

Fig. 1. Elution sequence of the anion exchange chemistry (Table 2) for a graywacke sample (GD) doped with laboratory Cd and Ag. The Cd data shown are from a separate experiment which provided a well-constrained Cd elution curve. Before concentration measurements, Rh was added to each fraction as an internal standard and the intensities of Zn, Ag, Cd and Sn ion beams were normalized to the ^{103}Rh ion beam to cancel out time-dependent variations in the uptake rate of the sample solutions. Palladium is not eluted and discarded with the resin.

tion. Thus, Ag must also be removed from the Cd fraction, because any Ag that is derived from the sample may have a fractionated isotope composition. Furthermore, the decay of extinct ^{107}Pd to ^{107}Ag could have generated radiogenic Ag isotope compositions in meteorite samples.

A two-stage column chemistry procedure was used in this study for the separation of Cd from geological matrices (Table 2). In the first stage, anion-exchange chromatography serves to separate Cd from most matrix elements (Fig. 1). The procedure largely follows published Cd separation protocols (Rosman and De Laeter, 1974; Loss et al., 1990), but an HNO_3-HBr mixture was used for the elution of Zn (Strelow, 1978).

The Cd fraction obtained from the anion-exchange separation still contains a substantial amount of Sn (Fig. 1). Therefore, Cd is separated from the residual Sn in a second column that exploits the high distribution coefficient of Sn between HCl and the Eichrom TRU Spec resin (Yi et al., 1995) (Table 2). This second step also separates Cd from any traces of Nb, Zr and Mo which avoids oxide- and nitride-based interferences of these elements on Cd and Ag isotopes (Table 1). After chemical separation, the Cd fraction was dried down repeatedly with a drop of concentrated HNO_3 to remove all Cl from the sample solutions.

The total procedural blank for Cd was determined by spiking the blank solutions with Rh as an internal standard. The Cd blanks were $\leq$20 pg Cd, except for two early blank determinations, which yielded up to 380 pg of Cd. However, no critical samples with low Cd contents were processed during this early stage. Since at least 5 ng of Cd were consumed in each analysis, a blank contribution of 20 pg is insignificant. Chemical yields and Cd isotope fractionation during Cd separation are discussed in sections 3.1.2.

2.2. Mass Spectrometry

2.2.1. Preparation of Sample and Standard Solutions for Analysis

The Cd obtained from the column chemistry was taken up in 300 μL of 0.05 mol/L HNO_3. To avoid systematic errors, sample and standard solutions were analyzed under similar conditions. The Cd ion beam intensities of the samples and the accompanying standards (which were used for normalization) were closely matched such that sets of sample Cd solutions with lower Cd concentrations were accompanied by a more diluted standard solution. Appropriate dilution factors for the samples were determined before the measurement session by the analysis of small sample aliquots (1/30) that were spiked with Rh as an internal standard.

To correct for the drift in the instrumental mass bias, both the sample and the Cd standard solutions were doped with Ag such that similar Cd/Ag ratios were obtained. Aliquots from a subset of samples were doped with Sb to verify the results from Ag-doping. Silver was sometimes found to be unstable in stored solutions. To ensure that both samples and standards have the same Ag concentrations and contain Ag of identical isotope composition, Ag was added on the day of measurement from the same bottle of a 1 ppm Ag (or Sb) working solution.

2.2.2. Instrumentation and Measurement Protocols

Most of the Cd isotope measurements were performed with the Nu Plasma MC-ICPMS instrument at the ETH Zürich (Belshaw et al., 1998; Rehkämper et al., 2001). A characteristic feature of the Nu Plasma is the combination of fixed Faraday collectors with variable dispersion zoom optics. A Cetac MCN 6000 desolvating nebulizer was employed for sample introduction. All isotope measurements were performed by static mul-

Table 3. Instrument parameters.

	Nu Plasma Zürich	IsoProbe Münster
RF power	1350 W	1320 W
Acceleration voltage	~4000 V	~6000 V
Mass analyser pressure	$\sim 2 \times 10^{-9}$ mbar	$\sim 2 \times 10^{-8}$ mbar
Nebuliser	Cetac MCN 6000	Cetac MCN 6000
Spray chamber temperature	75°C	75°C; 100°C[a]
Sample uptake rate	~100 μL/min	~100 μL/min
Extraction lens setting[b]		~−35% or ~+15%
Total signal intensities[c]	0.3–1.0 nA/ppm Cd	0.1–1.1 nA/ppm Cd
Transmission efficiency[c]	0.02–0.07%	0.01–0.07%
Mass discrimination[d]	1.7–2.3%/amu	2.1–2.7%/amu

[a] PFA spray chamber and nebuliser permit higher spray chamber temperatures which lowers memory effects.

[b] A positive potential can be applied to the collimator cone (the soft-extraction option) to reduce background peaks from contamination of the interface/hexapole tip region.

[c] The low transmission of 0.01% that occurred on the IsoProbe during some measurements is the net result of soft extraction, inefficient cones and the use of a PFA spray chamber/nebulizer. Together, these factors lower the transmission by a factor of ~6. For both instruments, the condition of the nebulizers, and the design and condition of the skimmer cones are largely responsible for the variable transmission.

[d] Relative to $^{110}Cd/^{114}Cd = 0.438564$ (Rosman et al., 1980a). IsoProbe: somewhat higher mass bias with soft extraction.

tiple collection with Faraday cups. Collector configurations and details of the instrument parameters are summarized in Tables 1 and 3.

The Cd content of most natural samples is rather low, but a certain Cd ion beam intensity is required for precise analyses. To yield sufficient ion beam intensities, data collection typically utilized only 40 or 45 integrations of 5 s each, in blocks of 20 or 15, respectively. On-peak baselines were measured for 20 s before each block, with the ion beam deflected in the electrostatic analyzer. With the Nu Plasma, the Ag isotope ratio cannot be measured together with ^{115}In and ^{117}Sn in a single measurement cycle. Hence, no correction of the Cd isotope ratios for isobaric interferences from In and Sn was possible during the main data acquisition sequence (termed "main run" hereafter). For each sample, the main run was therefore immediately followed by a separate measurement (termed "interference run"), which was used to determine the isobaric interferences of In and Sn on the various Cd isotopes (Table 1; details below). The zoom optics and the laminated magnet of the Nu Plasma enable fast switching from the main run to the interference run collector setting.

The ion beam intensity of ^{112}Cd was typically 0.2 to 1.2×10^{-11} A for rock and meteorite samples and 2 to 3×10^{-11} A for analyses of minerals and the VTA-3 Cd metal. The Ag (or Sb) concentrations of the solutions were adjusted, such that ion beam intensities of $\sim 3 \times 10^{-11}$ A were obtained for ^{107}Ag and ^{109}Ag. Washout of Cd from the MCN 6000 with 0.05 mol/L HNO_3 usually required < 5 min. While Cd was observed to wash out almost completely, a Ag signal of $\sim 1 \times 10^{-14}$ A typically built up during the course of a 5–12 h measurement session.

Additional Cd isotope measurements were carried out with a Micromass IsoProbe (e.g., Rehkämper and Mezger, 2000; Münker et al., 2001), either at the Universität Münster or at the Micromass factory in Manchester, UK. The IsoProbe is, in contrast to other MC-ICPMS instruments, a single-focusing mass spectrometer. Thermalization of the analyte ions in a hexapole collision cell serves to reduce the ion energy spread. For Cd isotope analyses, Ar gas was bled into the collision cell at a flow rate of ~1.2 mL/min. In most cases, a Sb solution was added to samples and standards and the $^{121}Sb/^{123}Sb$ ratio was used for the correction of the instrumental mass bias. Some IsoProbe measurements of VTA-3 Cd, however, utilized Ag for mass bias correction. Baselines were measured before each block for 20 s at half-masses at the high and low mass sides of peaks. Collector configurations and instrument parameters are given in Tables 1 and 3.

2.2.3. Data Presentation

All results are reported as εCd/amu, which is the deviation of the Cd isotope composition of a sample relative to the JMC Cd standard in parts/10,000, normalized to a mass difference of 1 atomic mass unit (amu):

$$\varepsilon\text{Cd/amu} = \left(\frac{(^{i}\text{Cd}/^{j}\text{Cd})_{\text{sample}}}{(^{i}\text{Cd}/^{j}\text{Cd})_{\text{std}}} - 1 \right) \times 10{,}000/(m_i - m_j) \quad (1)$$

Here, i and j refer to the isotopes of mass m_i and m_j. To conform with other stable isotope systems, where positive values usually refer to samples enriched in the heavy isotopes the $(m_i - m_j)$ term was introduced. This term also results in the per amu notation, which facilitates the comparison of data obtained for different Cd isotope ratios. It is important to note, however, that the εCd/amu values derived from different Cd isotope ratios are not identical, particularly for strongly fractionated samples. This is because natural mass fractionations are (approximately) a function of the mass difference between the isotopes i and j relative to the absolute mass. This relative mass difference is slightly larger between two "light" isotopes (e.g., for $^{110}Cd/^{111}Cd$) than between two heavier isotopes (e.g., for $^{113}Cd/^{114}Cd$). For example, a value of +30.0 εCd/amu based on $^{110}Cd/^{114}Cd$ yields only +29.7 εCd/amu based on $^{112}Cd/^{114}Cd$ (calculated with the exponential law). However, such differences are usually insignificant compared to the current measurement uncertainties.

2.2.4. Interference Corrections and Matrix Effects

Direct isobaric interferences on Cd isotopes can be generated by the elements Pd, In and Sn (Table 1). Some Sn and traces of In, but no Pd were found to be present in the Cd sample solutions. To correct for the isobaric interferences of Sn and In, the main Cd isotope ratio measurements were immediately followed by a separate interference run on the same solution. No separate interference run was needed for measurements with the IsoProbe MC-ICPMS, because In and Sn and Ag (or Sb) and Cd ion beams were collected simultaneously (Table 1). During the interference run, the ion beam intensities of ^{115}In and ^{118}Sn and the relevant Cd isotopes were measured. Interference-corrected Cd isotope ratios (R_{IR}) and Cd isotope ratios

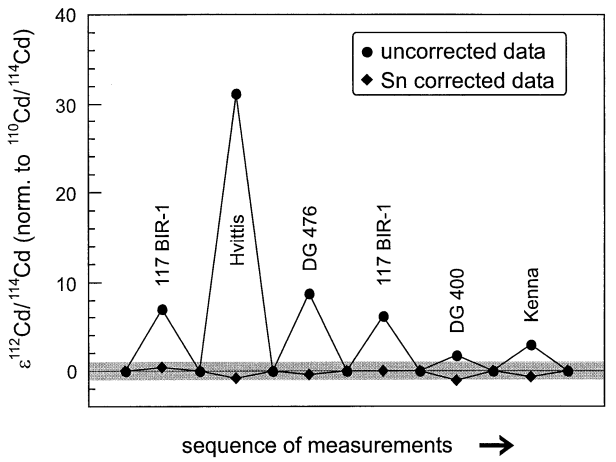

Fig. 2. Tin interference corrected and uncorrected Cd data in the sequence of measurements. Unlike elsewhere in the paper, the Cd data in this figure are internally normalized relative to $^{110}Cd/^{114}Cd$ using the exponential law. Internal normalization removes the effects of instrumental mass discrimination and natural isotope fractionation and thus allows to precisely evaluate the accuracy of the Sn interference correction. Sample measurements alternate with JMC Cd measurements (εCd/amu = 0) and both samples and standards yield the same isotope composition after Sn correction. The figure only shows results for samples with low Cd contents (5 to 10 ng Cd consumed per analysis), where Sn corrections are generally more significant, and also includes the sample with the largest Sn correction. Due to the low Cd content of the samples, only 20 ratios (10 ratios for Kenna) were obtained in the main run. The isotope composition of the samples deviates by not more than ± 1 εCd (per 2 amu; gray bar) from the bracketing JMC Cd measurements. During the interference run, the "true" Sn isotope composition (Lee and Halliday, 1995) was "mass biased" to simulate the instrumental mass bias that effects the interfering Sn. Because the ^{117}Sn and ^{118}Sn ion beams are too small to obtain a precise isotope ratio, the exponential law mass fractionation coefficient was calculated from Cd isotopes: $f = \ln(2.2443/^{111}Cd/^{114}Cd_{raw})/\ln[m(^{111}Cd)/m(^{114}Cd)]$, were m(^{111}Cd) is the mass of ^{111}Cd etc., and then applied to Sn isotope ratios, e.g., $^{112}Sn/^{118}Sn_{biased} = {}^{112}Sn/^{118}Sn_{true} \times [m(^{112}Sn)/m(^{118}Sn)]^{-f}$ (minus f, to reverse the correction). Hvittis, Kenna and DG (=Dar al Gani) refer to meteorite data that will be published elsewhere.

uncorrected for isobaric interferences (r_{IR}) are determined in the interference run. Both, R_{IR} and r_{IR} are uncorrected for instrumental mass discrimination. However, because Sn and In isotope ratios are affected by the large instrumental mass discrimination, a mass bias term was included to simulate the mass bias for the Sn and In isotope ratios that were used for the corrections (see Fig. 2 caption for details). From the interference run data, a correction factor F is calculated for each Cd isotope ratio:

$$F = R_{IR}/r_{IR} \quad (2)$$

and used for the offline correction of the results of the main run:

$$R_{MR} = F \times r_{MR} \quad (3)$$

R_{MR} and r_{MR} represent the interference corrected and uncorrected isotope ratios of the main run, respectively. This procedure was used for both the uncorrected and the Ag-normalized data of the main run. Indium corrections on mass 113 were $<$ 10 ppm, except for four samples, that required corrections of up to 35 ppm. Tin interferences on the $^{112}Cd/^{114}Cd$ ratio typically required corrections of $\sim$100 ppm, but even the sample with the largest Sn interference of $\sim$3000 ppm was accurately corrected (Fig. 2).

To identify other elements that may be present in the sample solutions following chemical separation of Cd, mass scans from 45 to 250 amu were obtained from a combination of different leftover sample solutions. Only traces of Zn, Ru, and Ba were observed to be present. Of these, Zn-argides and Ru-oxides and nitrides interfere with Cd and Ag isotopes (Table 1). Corrections for such molecular interferences are not possible and thus we investigated the effects of Ru and Zn additions to the standard solutions.

The addition of Ru to Cd-Ag standard solutions (Ru/Cd = 0.1 and 3.3) did not change the Ag-normalized (see next section) $^{112}Cd/^{114}Cd$ ratio by more than 0.7 εCd/amu and no changes in the mass bias due to Ru addition were detectable. However, in solutions with Ru/Cd = 33, all $^{i}Cd/^{114}Cd$ ratios showed a systematic bias of about -3 εCd/amu between Ag-normilized and bracketing data (see below). Furthermore different Cd isotope ratios also yielded inconsistent εCd/amu values that deviated from each other by up to 4 εCd/amu. The observed inconsistencies possibly result from a combination of matrix effects and molecular interferences.

Since no such effects were detected for solutions with Ru/Cd = 0.1 and 3.3, Ru/Cd ratios of up to 3 can be tolerated. The Ru/Cd ratios of the Cd fractions were found to be $<$ 0.1 for all samples presented here.

The interference of $^{67}Zn^{40}Ar^{+}$ on $^{107}Ag^{+}$ can generate Ag-normalized Cd isotope ratios that display an apparent enrichment of the heavy isotopes. Mixed Cd-Ag-Zn solutions with Zn/Ag ratios of 1.0 (Zn/Cd = 3.3) were observed to produce a systematic offset of $\sim$1.9 εCd/amu for all Cd isotope ratios. However, the maximum Zn/Ag ratio observed for the Cd fraction of a sample was $<$ 0.06, which can be expected to be negligible.

Errors due to matrix effects or peak tail contributions to neighboring masses could also result from the addition of variable amounts of Ag to the Cd sample solutions. The latter effect should be negligible in the mass region of interest for the IsoProbe (Münker et al., 2001) and especially for the Nu Plasma with its superior abundance sensitivity (Rehkämper and Mezger, 2000; Thirlwall, 2001). Furthermore, three sample solutions that were each analyzed twice, but with Ag/Cd ratios that differed by factors of $\sim$2 to 3, yielded identical results within uncertainty (Table 4).

Matrix effects typically produce deviations between data obtained by Ag-normalization procedures and standard-sample bracketing (see below). Spectral interferences result in εCd/amu values that are incompatible if they are calculated from different Cd isotope ratios. The few data that were inconsistent in these respects were therefore discarded.

2.2.5. Mass Bias Correction

The uncorrected raw isotope ratios reflect the mass discrimination of MC-ICPMS instruments, which preferentially transmit heavier ions. In the absence of systematic errors (e.g., interferences), the drift in mass bias should generate raw Cd isotope data that plot on mass fractionation lines in Cd three

Table 4. Cadmium stable isotope compositions.

MS[a]	Diss.[b]	Sample	εCd/amu[c]	ng Cd[d]
Carbonaceous chondrites				
Nu	I	Orgueil CI	−0.3	65
Nu	I	Orgueil CI	−0.7	65
Nu	91	Murchison CM2	0.9	45
Nu	A	Allende CV3	−0.2	40
Nu	35	Allende CV3	−0.9	45
Nu	35	Allende CV3	0.0	15
Nu	105	Allende CV3	0.2	45
Nu	105	Allende CV3	−0.7	45
Nu	128	Allende CV3	−0.9	45
Nu	128	Allende CV3	+0.3	45
Nu	116	Allende CV3	0.6	45
		Allende mean (n = 8)	−0.2 (1.1)	
Ordinary chondrites				
Nu	108	Semarkona LL3.0	−19.5	60
Nu	108	Semarkona LL3.0	−19.4	60
IP-M (Sb)	108	Semarkona LL3.0	−19.2	60
Nu	109	Bishunpur LL3.1	27.2	5
Nu	180	Bishunpur LL3.1	28.8	15
Nu	39	SQ 001 L/LL3[e]	36.6	250
Nu	39	SQ 001 L/LL3[e]	36.7	250
Nu	39	SQ 001 L/LL3[f]	35.0	250
Nu	39	SQ 001 L/LL3[f]	35.1	250
IP-M (Sb)	39	SQ 001 L/LL3	37.0	250
Nu	137	Dimmit H3.7	17.5	140
IP-M (Sb)	137	Dimmit H3.7	18.4	140
Nu	31	Brownfield H3.7[e]	27.6	140
Nu	107	Forest Vale H4	7.2	150
Nu	107	Forest Vale H4	8.3	150
IP-M (Sb)	107	Forest Vale H4	8.4	150
Rumuruti chondrite				
Nu	122	NWA 755 R3.7	6.8	105
Nu	122	NWA 755 R3.7	7.5	105
IP-M (Sb)	122	NWA 755 R3.7	7.9	105
Terrestrial rocks				
Nu	35	GD (graywacke)	1.3	95
Nu	35	GD (graywacke)	1.3	95
Nu	35	GD (graywacke)	1.9	95
Nu	104	GD (graywacke)	0.9	60
Nu	104	GD (graywacke)	0.9	60
Nu	22	GD (graywacke)	1.0	75
Nu	22	GD (graywacke)	2.0	75
Nu	126	GD (graywacke)	0.6	35
		GD mean (n = 8)	1.2 (1.0)	
Nu	34	TW (shale)	0.3	35
Nu	101	TW (shale)	0.3	40
Nu	102	NZ 404c (shale)	−1.2	90
Nu	11	NZ 404c (shale)	−0.9	80
Nu	11	NZ 404c (shale)	−0.9	80
Nu	103	BIR-1 (basalt)	0.1	15
Nu	13	BIR-1 (basalt)	−0.2	15
Nu	117	BIR-1 (basalt)[f]	1.2	25
Nu	117	BIR-1 (basalt)[f]	1.0	25
Nu	127	BIR-1 (basalt)	0.9	20
		BIR-1 mean (n = 5)	0.6 (1.3)	
Nu	21	DR-N (diorite)	−0.6	75
IP-M (Sb)	21	DR-N (diorite)	0.5	75
Impact-related rocks				
Nu	106	layered tektite	7.6	20
Nu	190	gn. bomb-core	0.1	250
Nu	190	gn. bomb-core	−0.5	250
Nu	190	gn. bomb-core	−0.4	250
Nu	191	gn. bomb-transition zone	−0.7	130
Nu	191	gn. bomb-transition zone	−0.6	130
Nu	191	gn. bomb-transition zone	−0.4	130
Nu	194	gn. bomb-melt coating	0.7	5
Nu	195	gn. bomb-host rock	0.0	25
Minerals				
Nu		$ZnCO_3$ (Tsuneb)[e] (n = 4)	0.2 (0.5)	
Nu		$CdCO_3$ (Tsuneb)[e] (n = 4)	0.0 (0.6)	
Nu		CdS (Moravica)[e] (n = 4)	1.0 (0.4)	
Nu		ZnS (Moravica)[e,f] (n = 4)	0.6 (0.5)	
Aragonite precipitation				
Nu	1	Arag. vs. Sol.	−1.6	
Nu	1	Arag. vs. Sol.	−1.7	
Nu	1	Arag. vs. Sol.	−1.5	
Nu	2	Arag. vs. Sol.	−1.5	
Nu		Arag. 1 vs. Arag. 2	0.7	
Nu		Arag. 1 vs. Arag. 2	0.2	
Nu		Arag. 1 vs. Arag. 2	0.2	
Second standard				
IP-M (Sb)		VTA-3 Cd (n = 4)	10.0 (0.8)	
IP-M		VTA-3 Cd (n = 3)	9.6 (0.2)	
IP-UK		VTA-3 Cd[e] (n = 4)	9.6 (0.4)	
Nu		VTA-3 Cd[e] (n = 13)	9.8 (0.6)	
Nu		VTA-3 Cd (n = 4)	9.5 (0.2)	
		VTA-3 mean (n = 28)	9.7 (0.6)	

Note: Uncertainties (in brackets): two standard deviations.

[a] Mass spectrometer; Nu = Nu Plasma, IP-M = Münster IsoProbe, IP-M (Sb) = Münster IsoProbe with Sb normalization, IP-UK= IsoProbe at Micromass Ltd. UK.

[b] The lab ID-numbers refer to separate dissolutions.

[c] Calculated based on $^{112}Cd/^{114}Cd$, except IP-M (Sb) data other than VTA-3 Cd are based on $^{110}Cd/^{114}Cd$. Positive values refer to heavy isotope compositions (see Eqn. 1).

[d] Estimated amount of Cd recovered from samples; often split among several analyses.

[e] No Sn correction applied, but correction is expected to be < 0.1 εCd/amu

[f] Samples analyzed with different Ag/Cd ratios.

Sample abbreviations: gn. = gneiss; NWA = North West Africa; SQ = Sarir Qattusah.

isotope plots (Fig. 3). The natural logarithms of the isotope ratios are used in Figure 3, because this produces linear fractionation trends (Maréchal et al., 1999). The samples and standards analyzed throughout this study fall onto the same fractionation line in a plot of $\ln(^{112}Cd/^{114}Cd)$ vs. $\ln(^{111}Cd/^{114}Cd)$ which indicates that the sample measurements are not significantly biased by spectral interferences. Similar results are obtained for other Cd three isotope plots (not shown) that involve the abundant isotopes (^{110}Cd, ^{111}Cd, ^{112}Cd, ^{113}Cd, ^{114}Cd).

If the instrumental mass discrimination is correctly described by the exponential law (Russel et al., 1978), the slope of the mass fractionation line in Figure 3 should be:

$$\text{slope} = \ln[m(^{112}Cd)/m(^{114}Cd)]/\ln[m(^{111}Cd)/m(^{114}Cd)] = 0.6641 \quad (4)$$

where $m(^{114}Cd)$ is the mass of ^{114}Cd, etc. For the Cd isotope ratios of Figure 3, the slope of the data is in accord with exponential law mass fractionation. Similar plots based on other Cd isotopes, however, have slopes that are in agreement with power law fractionation or slopes that are different from those expected for either of the two laws. Therefore, the long-term correlations do not provide constraints on which law best describes the instrumental mass discrimination. Likewise, Vance and Thirlwall (2002) found that the use of best-fit

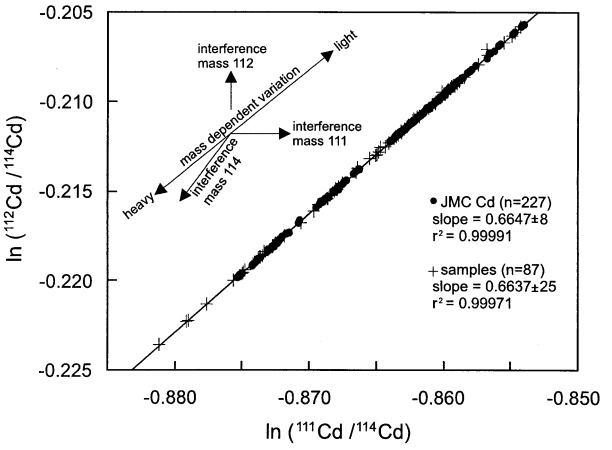

Fig. 3. Cadmium three isotope plot for JMC Cd and sample data obtained within 15 months. The natural logarithm of the raw data is plotted to linearize the fractionation curve. The variable instrumental mass discrimination generates strong correlations between two Cd isotope ratios. For samples, natural Cd isotope fractionation enhances the spread in the diagram. The sample data plots on the fractionation line defined by the JMC Cd data and the measured slopes of both, natural samples and JMC Cd coincide within uncertainty (95% confidence), proving the internal consistency of the results. The figure shows more samples than are discussed in this paper.

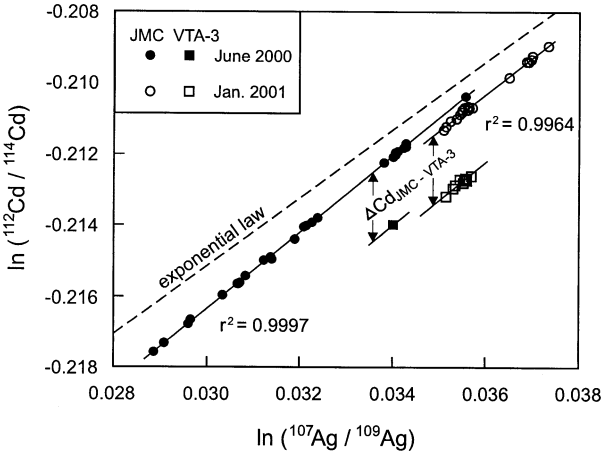

Fig. 4. Observed correlations between the raw isotope ratios of Cd and Ag from two measurement sessions. The offset between two standards (JMC Cd and VTA-3 Cd) at the Cd isotope axis corresponds to the relative Cd isotope fractionation (Maréchal et al., 1999). The dashed line denotes the slope predicted by the exponential law. This line is at an arbitrary position, i.e., no "true" Ag or Cd isotope compositions are assumed. The slopes defined by the raw Cd and Ag data are steeper than expected from the exponential law.

long-term correlations for the internal normalization of Nd isotope ratios yields inaccurate results.

The dispersion of the sample data along the mass fractionation line in Figure 3 is due to variations in both instrumental and natural mass-dependent isotope fractionation. To measure the natural isotope fractionation of a sample relative to the Cd isotope standard (JMC Cd) accurately, the raw data must be corrected for the drift in the instrumental mass bias. Three mass bias correction procedures, that have been used in previous studies were evaluated. (1) Standard-sample bracketing (e.g., Belshaw et al., 1998; Tomascak et al., 1999), where sample measurements are bracketed by standard measurements. The sample data are referenced to the mean result of the preceding and succeeding JMC Cd measurements. (2) External normalization with standard-sample bracketing (Rehkämper and Halliday, 1999; Carlson and Hauri, 2001). The exponential law is used to normalize the Cd isotope ratios relative to the $^{107}Ag/^{109}Ag$ ratio of admixed Ag. The Ag-normalized sample data are referenced to the mean value of the Ag-normalized standard measurements that bracket the sample analysis. Alternatively, Sb can be used for this purpose instead of Ag. (3) The empirical method of Maréchal et al. (1999) that is also based on external normalization to the $^{107}Ag/^{109}Ag$ ratio but relies on observed correlations between Cd and Ag isotope ratios rather than correlations predicted by the exponential law.

If the instrumental mass discrimination of Cd and Ag isotopes follows the exponential law, the raw isotope ratio data should define a fractionation line in $\ln(^iCd/^jCd)$ vs. $\ln(^{107}Ag/^{109}Ag)$ isotope space, with a slope that can be calculated using an equation similar to Eqn. 4. The Cd-Ag data, however, defines correlation lines with slopes that do not agree with the exponential (or power) law mass fractionation that would be expected, if both elements experienced exactly the same mass discrimination (Fig. 4). Furthermore, the slopes were observed to vary significantly between measurement sessions. Similar observations have been made previously for other element pairs (Maréchal et al., 1999; White et al., 2000; Anbar et al., 2001).

If the instrument settings are left unchanged during one measurement session, the data for multiple standard measurements fall onto well-defined correlation lines, that are produced by the drift of the instrumental mass discrimination. The empirical method of Maréchal et al. (1999) employs this correlation for the correction of the instrumental mass discrimination. A linear regression is fitted to the raw data obtained for the JMC Cd standard in $\ln(^iCd/^jCd)$ vs. $\ln(^{107}Ag/^{109}Ag)$ isotope space. For both, standards and samples, the slope of this regression line relates the raw and fractionation-corrected (corr) Cd isotope ratio to the raw Ag isotope ratio and the Ag isotope reference value (ref):

$$\text{slope JMC Cd} = \frac{\ln(^iCd/^jCd)_{raw} - \ln(^iCd/^jCd)_{corr}}{\ln(^{107}Ag/^{109}Ag)_{raw} - \ln(^{107}Ag/^{109}Ag)_{ref}} \quad (5)$$

Eqn. 5 can be rearranged into:

$$(^iCd/^jCd)_{corr} = (^iCd/^jCd)_{raw} \times \left(\frac{(^{107}Ag/^{109}Ag)_{ref}}{(^{107}Ag/^{109}Ag)_{raw}}\right)^{\text{slope JMC Cd}} \quad (6)$$

Eqn. 6 was used for the normalization of the raw standard and sample Cd isotope ratios to a common reference value $(^{107}Ag/^{109}Ag)_{ref}$. The choice of the Ag reference value is arbitrary for relative measurements (ε-notation), because samples and standards are corrected along parallel trajectories (Fig. 4). The natural mass fractionation of a sample relative to the corrected mean value of the JMC Cd standard was then calculated following Eqn. 1.

Results obtained with the three mass bias correction proce-

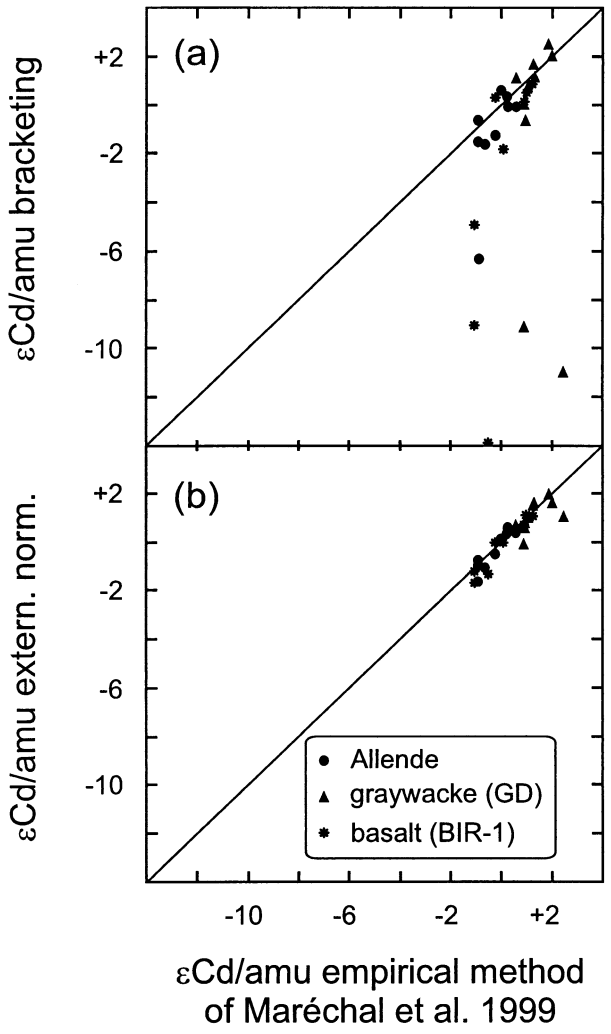

Fig. 5. a and b. Comparison of results from different normalization procedures for repeated measurements of a graywacke (GD), a basalt (BIR-1) and a meteorite sample (Allende): (a) comparison of data corrected by the bracketing method from data corrected by the empirical method of Maréchal et al. (1999), (b) comparison between external normalization and the empirical method (both employ Ag isotopes). Bracketed data from one batch of chemistry produced several matrix-induced outliers that yield much better results if normalized to Ag isotopes.

dures are compared in Figure 5. Data are shown for multiple measurements of three samples, the Allende meteorite, graywacke GD and basalt BIR-1. The Cd isotope results obtained by external normalization and by the empirical method all agree to within better than ± 2 εCd/amu (Fig. 5b). The differences between data collected by standard-sample bracketing and the empirical method are larger in general. In addition, standard-sample bracketing produced several outliers with low εCd/amu values (Fig. 5a). It is noteworthy that these outliers were all from the same batch of column chemistry and that Cd isotope ratios other than $^{112}Cd/^{114}Cd$ were also anomalous. This indicates that the outliers were generated by a matrix-related mass bias effect, probably because the column chemistry did not produce sufficiently clean Cd cuts.

The outliers show only small offsets relative to mean values if corrected by either external normalization or the empirical method. This demonstrates that the two Ag normalization procedures are less susceptible to matrix effects than simple standard-sample bracketing. To ensure that the data quality is not compromised by matrix effects, we rejected all sample data that showed deviations of >3 εCd/amu between results obtained by standard-sample bracketing and the empirical method of Maréchal et al. (1999).

After rejection of the outliers, all three correction procedures yield consistent results. The comparison of the standard-sample bracketing with the empirical method yields a mean offset of -0.3 ± 1.4 εCd/amu (2 sd = 2 standard deviations). The mean offset between the empirical method and external normalization is 0.0 ± 0.5 εCd/amu (2 sd). The consistency of the results obtained with different procedures for mass discrimination correction supports the conclusion that all three techniques generate accurate results. Here, the Cd isotope ratios that are obtained by the empirical method of Maréchal et al. (1999) are preferred over external normalization, (1) because they have slightly better reproducibilities, and (2) because the exponential law does not accurately describe the relative mass discrimination of Cd vs. Ag isotopes (Fig. 4). External normalization, however, is simpler in its application and can therefore provide a suitable alternative to the empirical method of Maréchal et al. (1999).

3. RESULTS AND DISCUSSION

3.1. Precision and Accuracy

After correction for isobaric interferences and mass discrimination, the samples yield consistent εCd/amu results for $^{110}Cd/^{114}Cd$, $^{111}Cd/^{114}Cd$, $^{112}Cd/^{114}Cd$ and $^{113}Cd/^{114}Cd$. The $^{112}Cd/^{114}Cd$ data, however, display the best long-term reproducibility. Therefore, the εCd/amu values in Table 4 and Figures 5 to 10 are based on the $^{112}Cd/^{114}Cd$ ratio. The only exception are the Sb-normalized IsoProbe data for all samples except VTA-3 Cd, where εCd/amu was calculated from $^{110}Cd/^{114}Cd$ because ^{112}Cd was not measured. Although the lighter Cd isotopes make up the numerators, positive εCd/amu values always denote heavy Cd isotope compositions (Eqn. 1).

3.1.1. Standard Solutions

Following mass discrimination correction by the empirical method of Maréchal, the data obtained for multiple analyses of the JMC Cd standard (interspersed between sample measurements) in one measurement session typically have a precision of ± 0.3 to ± 0.7 εCd/amu (2 sd). The reproducibility is generally better if the samples that are measured in this session have high Cd concentrations and therefore lower matrix contents due to dilution.

The Cd isotope composition of the fractionated VTA-3 Cd standard was determined relative to JMC Cd (Fig. 6, Table 4). The isotope ratios were measured with three different MC-ICPMS instruments, the Nu Plasma in Zürich and the IsoProbe in Münster and Manchester. Some of the Münster measurements were normalized to Sb isotopes. All measurements of the VTA-3 Cd solutions yield very similar results, with an average of 9.7 ± 0.6 εCd/amu (2 sd). The fact that data acquired with

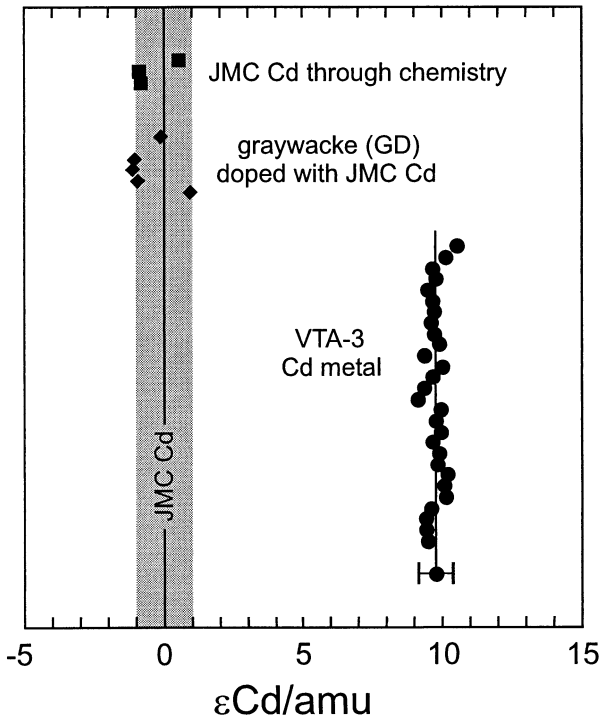

Fig. 6. Cadmium stable isotope compositions of standard solutions, including results for JMC Cd processed through chemistry with and without a rock matrix (gray bar: ± 1 εCd/amu). Repeated measurements of a fractionated Cd metal (VTA-3 Cd) obtained from different instruments and normalized to either Ag or Sb isotopes (Table 4) yield 9.7 ± 0.6 εCd/amu.

different instruments and different normalization protocols show such good agreement, indicates that the results are accurate within the given uncertainty.

3.1.2. *Cadmium Isotope Fractionation during Chemical Purification*

To test for Cd loss during the chemical separation procedure, eluate fractions collected before and after the Cd elution from the anion exchange resin were occasionally analyzed. These fractions always contained ⩽1% of the total Cd. Furthermore, a large meteorite sample (~600 mg) was processed through the anion-exchange column and all eluate fractions, except for the Cd fraction, were collected. This matrix fraction was then again passed through the anion-exchange chemistry. The Cd fraction that was collected from the second pass yielded only a typical Cd blank of ~10 pg. Thus no Cd loss occurred during the column separation, even though the column was loaded with a sample that was larger than usual (600 mg vs. the typical 100–500 mg). This suggests that Cd isotope fractionation during the anion exchange procedure could only occur if some Cd remains on the resin irretrievably.

To assess the possible extent of Cd isotope fractionation during partial elution, JMC Cd was processed with the anion-exchange chemistry (50 μg Cd) and in another experiment with the TRU-spec resin chemistry (10 μg Cd). Sequential eluate

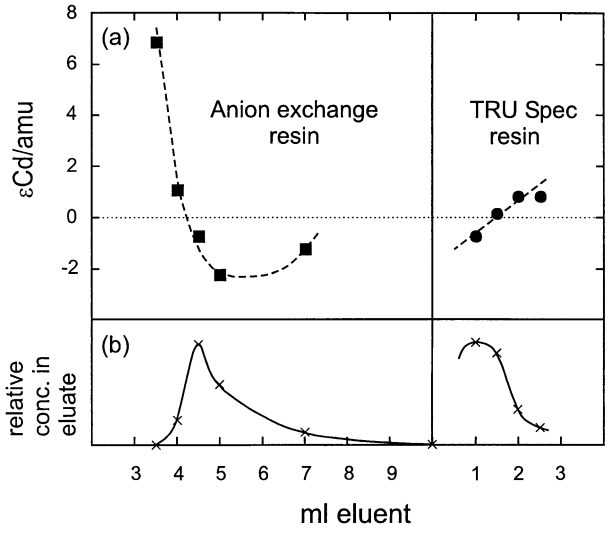

Fig. 7. Cadmium isotope compositions of sequentially eluted fractions collected from the two column chemistries. The measured Cd isotope composition is plotted versus the amount of eluent used (TRU Spec resin: 8 M HCl, anion exchange resin: 2 M HNO_3). The shapes of the corresponding elution curves are given for comparison. A curved fractionation trend is observed for the anion exchange separation step. The experiment with the TRU Spec resin corresponds to an earlier procedure, where all steps were carried out in 8 M HCl and 500 μL resin were used.

fractions that cover the complete elution of Cd were collected in these experiments.

The anion exchange chemistry produced a total fractionation range of ~9 εCd/amu (Fig. 7). However, the fraction with the heaviest Cd isotope composition (+6.9 εCd/amu) contained only ~0.01% of the total Cd. It is surprising that the last Cd fraction collected from the anion-exchange chemistry does not follow the trend of the earlier fractions, which display decreasing εCd/amu values during the elution. This behavior, which was reproduced in a second experiment, may be due to the presence of different Cd species (e.g., Cd complexes) with different distribution coefficients and fractionation factors between the solution and the resin. Cadmium species with such different behavior may result from the different eluents (HCl, HNO_3 and HBr) that are used in the anion exchange procedure. The integrated Cd isotope composition of the anion-exchange fractions corresponds to −1.0 εCd/amu for a total Cd yield of ~98% (using Rh as an internal standard). Within the uncertainty of the mass balance and the measurements, this result is close to the expected result of εCd/amu = 0.

For the TRU Spec chemistry, only limited Cd isotope fractionation (~1.5 εCd/amu) was detected (Fig. 7). This result is not surprising, given the limited adsorption of Cd onto this resin. Mass balance calculations show that the integrated isotope composition of Cd in the eluate is identical to unprocessed JMC Cd.

To ascertain that the separation procedure does not generate fractionated Cd isotope compositions in the Cd cuts, three aliquots of JMC Cd were processed through the complete column chemistry. In two further experiments, ~300 mg of rock powder (graywacke GD) were doped with 10 and 50 μg JMC Cd. The Cd isotope compositions ranged from −0.9 to

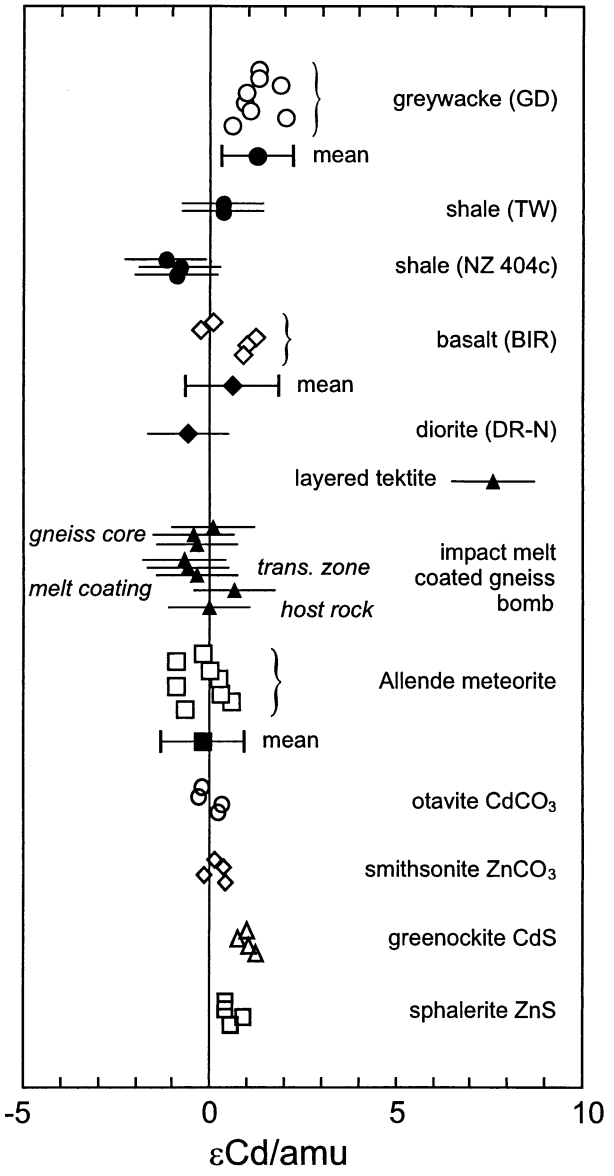

Fig. 8. Cadmium stable isotope compositions for rocks, minerals and the Allende meteorite. The Allende meteorite and the terrestrial samples show only small variations in isotope compositions, with the exception of a layered tektite sample that is enriched in the heavy Cd isotopes.

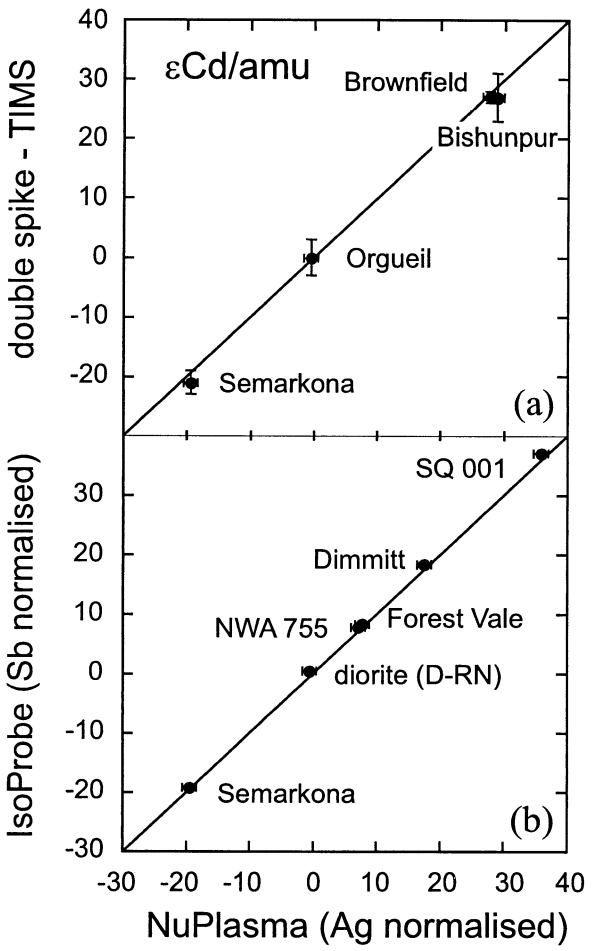

Fig. 9. a and b. Comparison of Cd stable isotope compositions of meteorite and rock samples determined by different instruments and methods. (a) Ag-normalized Nu Plasma data agrees within uncertainty with previously published double spike-TIMS data (Rosman et al., 1980a; Rosman and De Laeter, 1988; TIMS uncertainties were adopted from original papers). (b) Sb-normalized IsoProbe data obtained from the same measurement solution agrees well with Ag-normalized Nu Plasma data. NWA = North West Africa; SQ = Sarir Qattusah.

+0.5 εCd/amu (n=3; n is the number of measurements) for the matrix-free JMC Cd sample and from −1.1 to +0.9 εCd/amu (n=5) for JMC Cd with the graywacke matrix (Fig. 6).

Two main conclusions can be drawn from these results. (1) The isotope compositions of JMC Cd processed through the column chemistry are, within about ±1 εCd/amu, identical to the expected result (εCd/amu = 0). This indicates that the chemical separation does not produce any systematic bias. The similarity of the results obtained for JMC Cd with and without matrix furthermore shows that the presence of the graywacke matrix did not compromise the separation of Cd significantly. (2) The chemical separation of Cd, however, appears to slightly compromise the reproducibility of the data compared to results obtained for pure Cd standard solutions. This conclusion follows from the observation that multiple analyses of unprocessed Cd solutions (JMC Cd within single measurement sessions or VTA-3 Cd vs. JMC Cd on multiple days) display reproducibilities of about ±0.5 εCd/amu, whereas processed JMC Cd has a reproducibility that is about two times worse. This difference is possibly due to matrix effects from elements or organic species derived from the chemical separation procedure.

3.1.3. Reproducibility and Accuracy of Cd Data for Rocks and Meteorites

Three silicate samples were repeatedly analyzed over a period of several months during this study: the USGS standard reference basalt BIR-1 (97 ppb Cd; Yi et al., 1998), graywacke GD (250 ppb Cd; H. Heinrichs, personal communication), and the Allende meteorite (~220 ppb Cd; Rosman and De Laeter,

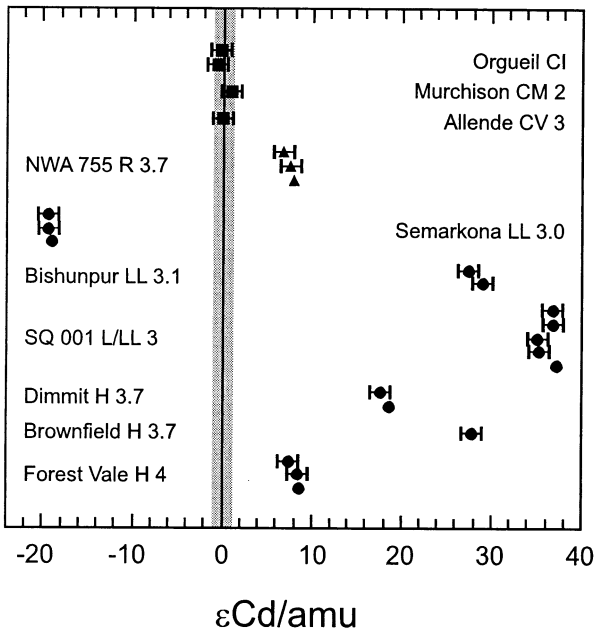

Fig. 10. Cd stable isotope compositions of chondritic meteorite samples (IsoProbe data without uncertainties). The gray bar denotes the variation observed in terrestrial rocks and minerals (excluding the layered tektite). No isotope fractionation is resolved between the carbonaceous chondrite samples and the Earth. In contrast, all ordinary chondrites and the Rumuruti chondrite have fractionated Cd isotope compositions. NWA = North West Africa; SQ = Sarir Qattusah.

1974; Loss et al., 1984). Repeated Cd isotope measurements from multiple digestions and separations yielded reproducibilities of ±1.3, ±1.0 and ±1.1 εCd/amu (2 sd), respectively (Table 4, Fig. 8). The average deviation (2 sd) for all BIR-1, graywacke and Allende data from the respective mean value is ±1.1 εCd/amu. This value is adopted as a realistic external reproducibility for rock and meteorite samples. Each of the five analyses of BIR-1 consumed only ~10–20 ng of Cd. The Cd isotope measurements for GD and Allende were typically performed with 20–30 ng of Cd per measurement. Other sample analyses consumed between 15 and 50 ng of Cd. Two analyses, for the Bishunpur chondrite and for a melt coating from a gneiss bomb, however consumed only 5 ng of Cd. Nonetheless, both results agree with the other Bishunpur and gneiss bomb results within the analytical uncertainty of ±1.1 εCd/amu (Table 4).

A comparison of Cd stable isotope data acquired for terrestrial rocks and meteorites with different instruments and measurement techniques is presented in Figure 9. Meteorite data obtained in this study (using the empirical method of Maréchal et al., 1999) is compared with previously published results acquired by TIMS and the double spike method (Rosman et al., 1980a; Rosman and De Laeter, 1988) in Figure 9a. The results for all four meteorites agree within uncertainty, and this demonstrates (1) that both studies used Cd reference standards (for the definition of εCd = 0) with identical or very similar Cd isotope compositions, (2) that the new MC-ICPMS methods generate accurate data for samples and (3) that the Cd isotope compositions of these meteorites are homogeneous at the scale of the analyzed samples. For a fifth meteorite sample, the ordinary chondrite Dimmitt, the data acquired in this study (+18 εCd/amu) is very different from the TIMS results, (−3 ± 4 εCd/amu; Rosman and De Laeter, 1978). Rosman and De Laeter (1974) obtained a Cd concentration of 44 ppb for Dimmitt, but our estimate of ~200 ppb is significantly higher. These discrepancies may be due to the analysis of sample splits with different lithologies. This is likely because Dimmitt is a regolith breccia that contains 30 to 50% of H4 and H5 chondrite clasts (Rubin et al., 1984).

Six meteorite samples and the diorite DR-N (a standard reference material from CRPG-CNRS/France) were analyzed with both the Nu Plasma (using the empirical method with Ag isotopes) and the IsoProbe (using the empirical method with Sb isotopes). Again, the results obtained with both methods agree within the external uncertainty of ±1.1 εCd/amu (Fig. 9b). This suggests that the reported Cd isotope data is accurate within the quoted uncertainty.

3.2. Cadmium Isotope Fractionation in Nature

3.2.1. Carbonates and Sulfides

The minerals smithsonite ($ZnCO_3$), otavite ($CdCO_3$) and greenockite (CdS) form during weathering processes at low temperatures. Nonetheless, these minerals and a sphalerite (ZnS) display total Cd isotope variations of only about ±1 εCd/amu, which is insignificant given the analytical uncertainty (Fig. 8, Table 4). This suggest that natural (inorganic) processes may be unable to generate substantial Cd isotope variations, even at low temperatures.

An aragonite sample that was precipitated in the laboratory at 10°C, with an experimental setup similar to that of Dietzel and Usdowski (1996) (performed by M. Dietzel; TU Graz, Austria) and the dissolved Cd that remained in the solution (ca. 86% of initial Cd) were analyzed for their Cd isotope compositions. To avoid the propagation of uncertainties (that would result if the aragonite and the dissolved Cd were first measured relative to JMC Cd), the aragonite sample was measured relative to the dissolved Cd (Table 4). To ascertain the results, Cd was chemically isolated from two separate aliquots of both the aragonite sample and the solution. Both aragonite aliquots displayed a light Cd isotope composition with εCd/amu ~ −1.5, relative to the Cd remaining in solution. This result is outside the external reproducibility of ±1.1 εCd/amu established for the analysis of rocks relative to JMC Cd and therefore probably meaningful. Furthermore, measurements of the two aragonite aliquots relative to each other revealed no significant offset (Table 4). The same aragonite sample was also analyzed for Ca isotope compositions, and the light Ca isotopes were enriched in the carbonate relative to the dissolved Ca (Gussone et al., 2003). Because Cd^{2+} substitutes for Ca^{2+} in aragonite, the observation that both Cd and Ca have light isotope compositions in the precipitate is consistent.

3.2.2. Sedimentary and Igneous Rocks

Three measurements obtained for two separate digestions of the Cambrian shale sample (NZ 404c) display light Cd isotope compositions outside the range measured for the graywacke sample (GD) (Fig. 8, Table 4). Therefore the resolvable difference between the two sedimentary rocks provides first evidence

for small terrestrial Cd isotope variations in low temperature environments. Resolvable isotope fractionation of Cd is not expected to occur during the formation of igneous rocks, because of the high temperatures involved. Mantle-derived igneous rocks may therefore be most suitable for estimating the Cd isotope composition of the bulk silicate Earth. The mantle-derived basalt BIR-1 from Iceland has a Cd isotope composition that is indistinguishable from the JMC Cd standard. Furthermore, the data for other terrestrial rocks and minerals scatter closely around εCd/amu $\approx$ 0. Therefore, the bulk silicate Earth most likely has a Cd isotope composition that is very similar to the JMC Cd standard with εCd/amu $\approx$ 0.

3.2.3. Impact-Related Rocks and Isotope Fractionation during Evaporation

The most fractionated Cd isotope composition for a terrestrial rock was identified for a layered (or Muong-Nong type) tektite from Laos, which displays εCd/amu = +7.6. The observation that none of the other terrestrial samples display such strongly fractionated isotope compositions, suggests that the heavy isotope composition of the tektite is due to the preferential loss of light Cd isotopes by evaporation during tektite formation. Previous stable isotope studies for K and Mg did not resolve any mass-dependent isotope fractionations in tektite samples (Esat, 1988; Humayun et al., 1994). Cadmium, however, is much more volatile than K and Mg. Therefore, a significant fraction of the initial Cd may have been volatilized during tektite formation, while K and Mg were retained and this could explain why only Cd isotopes show resolvable isotope fractionations.

Kinetic isotope fractionation during evaporation can be described with the Rayleigh equation,

$$\frac{(^{112}\mathrm{Cd}/^{114}\mathrm{Cd})_{\mathrm{residue}}}{(^{112}\mathrm{Cd}/^{114}\mathrm{Cd})_{\mathrm{initial}}} = f^{(\alpha_{\mathrm{kin}}-1)} \quad (7)$$

where f is the mass fraction of the residual Cd and α_{kin} is the kinetic isotope fractionation factor:

$$\alpha_{\mathrm{kin}} = (^{112}\mathrm{Cd}/^{114}\mathrm{Cd})_{\mathrm{vapor}}/(^{112}\mathrm{Cd}/^{114}\mathrm{Cd})_{\mathrm{residue}} = \sqrt{\mathrm{m}(^{114}\mathrm{Cd})/\mathrm{m}(^{112}\mathrm{Cd})} = 1.00890 \quad (8)$$

Cadmium forms a monatomic vapor (Chizhikov, 1966) and thus there are no complications concerning the mass of the evaporating species. Ideal Rayleigh evaporation requires that the vapor is instantaneously removed from the surface of the remaining reservoir and that the isotope composition of the residue remains homogeneous (Esat, 1996; Young et al., 1998; Wang et al., 1999; Nagahara and Ozawa, 2000; Ozawa and Nagahara, 2001). The latter condition is fulfilled if the evaporation rate is small compared to the rate of Cd diffusion in the remaining reservoir. In contrast to kinetic Rayleigh fractionation, equilibrium isotope fractionation between Cd in the vapor phase and Cd in the condensed phase is temperature-dependent and therefore probably insignificant in most cases.

The Cd content of the tektite was estimated to be ~11 ppb. The precursor material for the layered tektites were sediments with a chemical composition similar to the upper continental crust (Wasson, 1991; Koeberl, 1992). Such sediments can be assumed to have between 40 and 200 ppb Cd (Heinrichs et al., 1980). From this, it can be estimated that the tektite sample was depleted in Cd by a factor of 4 to 18 by evaporation. Inserting these depletion factors into Eqn. 7 indicates that the Cd isotope fractionation observed for the tektite is only 6 to 13% of the fractionation expected for ideal Rayleigh evaporation. Hence, the Cd isotope fractionation during tektite formation was strongly suppressed. This can be explained by (1) partial equilibrium between Cd in the gas phase and melt and/or (2) slow diffusion of Cd within the molten tektite precursor during evaporation. The latter explanation requires that chemical and isotope fractionation are decoupled, which may be possible for very volatile elements (Ozawa and Nagahara, 2001). Diffusion is rapid in liquids, and thus the homogenization of Cd isotopes will only be problematic if the melt volume is large (Young, 2000) and mixing by convection is slow. Young (2000) estimated that the suppression of K isotope fractionation during evaporation requires melt pools that measure several tens of centimeters. The tektite sample has a diameter of only ~4 cm, but Wasson (1991) suggested that the layered tektites are the remains from a extensive melt sheet or pool. Alternatively, partial equilibrium may have been established between the tektite melt and volatilized Cd, for example in gas bubbles that formed within the melt.

In addition to the tektite, we analyzed a gneiss bomb from the Popigai impact crater (Siberia), that is coated with layers of solidified impact melt. Different domains that were separated from this sample include (from inside to outside) the gneiss core, the transition zone, the melt coating and the surrounding host rock (Kettrup et al., 2003). Both the host rock (a clastic impact breccia) and the melt coating display low Cd concentrations (~20–30 ppb) compared to the core and the transition zone of the gneiss bomb (~90 ppb Cd). Despite of this apparent depletion, none of the samples display any significant Cd isotope fractionation. The observation that loss of Cd is not accompanied by resolvable isotope fractionation is probably best explained by a mixture of material that completely lost its original Cd inventory by melting or vaporization and material that remained solid and lost no (or little) Cd. It has been argued, that the melt coatings resulted from the accretion of hot impact melt droplets onto the cold gneiss bombs (Masaitis and Deutsch, 1999; Kettrup et al., 2003). It is likely that the impact melt droplets were initially devoid of Cd. In this case, the isotopically normal Cd of the melt coatings may have been derived from accreted dust, from the gneiss bomb interiors, or from the host rock. Nevertheless, the apparently depleted host rock and melt coating may also contain some material that was partially depleted in Cd. If the Cd isotope fractionation during partial depletion was suppressed, as suggested for the layered tektite, a contribution of depleted material in the percent range may not be resolvable.

3.2.4. Carbonaceous Chondrites

Variations of elemental abundances in chondrites and bulk terrestrial planets are strongly controlled by volatility. The relative abundances of most elements in CI carbonaceous chondrites such as Orgueil are considered to represent the composition of the primitive solar nebula. In contrast to CI chondrites, CM (Murchison) and CV (Allende) chondrites display decreasing abundances of moderately volatile elements with decreas-

ing condensation temperatures (Palme et al., 1988). The cause of the volatile element depletion is still under debate, but it may be due to either incomplete condensation from a hot solar nebula (Wai and Wasson, 1977; Humayun and Clayton, 1995) or evaporative loss of volatile elements during chondrule formation (Larimer and Anders, 1967; Anders et al., 1976; Wolf et al., 1980). The abundances of highly volatile elements (and moderately volatile elements with $T_C < 700$ K) in carbonaceous chondrites, however, have also been explained by a two-component mixture of a refractory component devoid of highly volatile elements and a primitive (matrix) component with initial abundances of highly volatile elements (Larimer and Anders, 1967; Wolf et al., 1980). In this case, no Cd isotope fractionation is expected for Cd depleted carbonaceous chondrites.

Within analytical uncertainty, the carbonaceous chondrites Orgueil, Murchison, and Allende have identical Cd isotope compositions (Fig. 10, Table 4), in spite of the large differences in Cd concentrations. The Cd abundances of Orgueil, Murchison, and Allende are 710 ppb, 440 ppb, and 220 ppb, respectively (Rosman and De Laeter, 1974; Loss et al., 1984; Rosman and De Laeter, 1988). The Cd isotope composition of the Earth also seems to be identical to that of the carbonaceous chondrites. McDonough (1999) inferred a bulk Earth concentration of 80 ppb Cd.

The Cd isotope data imply that the depletion of Cd (and by analogy of other highly volatile elements) did not involve significant Rayleigh evaporation. For the Earth and for Allende, more than 2% of Cd loss due to Rayleigh evaporation would result in detectable Cd isotope fractionation, for Murchison this limit is 8% (calculated from Ti normalized Cd concentrations).

The absence of Cd isotope fractionation in carbonaceous chondrites is consistent with the two-component mixing model that has been advocated for the highly volatile elements (Larimer and Anders, 1967; Wolf et al., 1980). However, the depletion of the moderately volatile element K cannot be explained by the two-component model alone and did not result in K isotope fractionation (Humayun and Clayton, 1995). Thus, while the absence of Cd isotope fractionations in carbonaceous chondrites can be explained by the two-component mixing model, it cannot be ruled out that Cd and K depletions are both due to another processes without isotope fractionation.

Palme (2001) suggested that the moderately volatile element depletion patterns in carbonaceous chondrites and in the Earth are similar. The identical Cd isotope compositions for the Earth and the carbonaceous chondrites may indicate that in both cases the same process is responsible for the depletion of the highly volatile elements. At least, it can be inferred that secondary loss of Cd from the Earth, for example during the Moon-forming impact, was either insignificant or did not involve Rayleigh fractionation.

3.2.5. Ordinary and Rumuruti Chondrites

The largest Cd stable isotope variations in this study were identified for unequilibrated ordinary chondrites, in accordance with the results of Rosman and coworkers (Rosman and De Laeter, 1976; Rosman et al., 1980b; Rosman and De Laeter, 1988). For these meteorites, the Cd isotope fractionation varies between -19 and $+36$ εCd/amu (Table 4, Fig. 10). Furthermore, we provide the first evidence for Cd isotope fractionation in a slightly metamorphosed ordinary chondrite (Forest Vale H4) and in an unequilibrated Rumuruti chondrite (North West Africa 755 R3.7). Both meteorites have εCd/amu values of about $+8$.

As pointed out by Rosman and De Laeter (1988), there is no obvious correlation between the magnitude or sign of the Cd isotope fractionation and the petrologic type (3.0–4) or group (H, L, LL). Semarkona, the only known ordinary chondrite of type 3.0, is unique because it has a light Cd isotope composition and the highest Cd concentration (1248 ppb Cd; Rosman and De Laeter, 1988) ever measured for a meteorite sample.

The depletions of moderately volatile elements (e.g., Zn) are uniform in ordinary chondrites of all petrological types. The distribution patterns of Cd and other highly volatile elements in ordinary chondrites are more complex. The Cd concentrations of metamorphosed ordinary chondrites are variable, but generally low, e.g., < 10 ppb in most H 4–6 ordinary chondrites (Wolf and Lipschutz, 1998). In unequilibrated ordinary chondrites, Cd and other highly volatile elements show both very low and very high concentrations that can exceed those of CI chondrites (Anders and Grevesse, 1989). The uniformly depleted moderately volatile elements S, K and Zn display no or rather small isotope fractionations in ordinary chondrites (Gao and Thiemens, 1993; Humayun and Clayton, 1995; Luck et al., 2001; Luck et al., 2002). This suggests that the large Cd isotope fractionations in ordinary chondrites are related to the complex distribution patterns of the highly volatile elements.

The Cd isotope fractionations can therefore be used to constrain the origin of the heterogeneous distribution of Cd and other highly volatile elements in ordinary chondrites. Two main explanations have been proposed: (1) redistribution during open-system thermal metamorphism (Dodd, 1969) and (2) primary equilibrium condensation. The latter model proposes that the low-temperature (matrix) component of those ordinary chondrites that were later metamorphosed inside the parent bodies accreted when the ambient nebula temperatures were still too high to condense large fractions of highly volatile elements. The unequilibrated ordinary chondrites are thought to contain a low-temperature component that experienced slightly lower nebula temperatures and thus contains higher abundances of highly volatile elements (Larimer and Anders, 1967; Keays et al., 1971; Laul et al., 1973; Larimer, 1973; Morgan et al., 1985).

It has furthermore been suggested that shock heating remobilized some highly volatile elements (see, e.g., Lipschutz and Woolum, 1988). Most of the ordinary chondrites and the single Rumuruti chondrite that were analyzed in this study are very weakly shocked (S2), whereas Dimmitt is weakly shocked (S3). Up to shock stage S2, there is no loss of noble gases or melt formation (Stöffler et al., 1991), and it is therefore unlikely that shock metamorphism is responsible for the observed Cd isotope fractionations in the samples of the present study. In addition, shock metamorphism is not expected to generate the observed differences in Cd abundances between unequilibrated and metamorphosed ordinary chondrites.

The Cd isotope data also appears to be inconsistent with partial equilibrium condensation as the cause of the observed highly volatile element distribution in ordinary chondrites. Even if partial condensation of Cd would have been accompa-

nied by equilibrium isotope fractionation, the fractionations would probably be smaller than observed. Furthermore, partial equilibrium (and kinetic) condensation should not result in the enrichment of light Cd isotopes in the condensed fraction as observed for Semarkona and also fails to explain highly volatile element concentrations that exceed those of CI chondrites (Anders and Grevesse, 1989). Therefore, the heterogeneous distribution patterns of highly volatile elements and the associated Cd isotope fractionations in ordinary chondrites are most likely due to a process other than primary partial condensation.

Open system thermal metamorphism is thus the most likely cause. Probably, Cd and other highly volatile elements were volatilized from the hot portions of the parent bodies during thermal metamorphism. The volatilized Cd then migrated along thermal and pressure gradients and finally recondensed in the cooler unequilibrated parts of the parent bodies. This scenario can account for the highly volatile element depletion of the metamorphosed ordinary chondrites, for the variable enrichments and depletions in the unequilibrated ordinary chondrites and is also capable to generate large Cd isotope fractionations. The heavy and light Cd isotope compositions may result from repeated partial evaporation and condensation of Cd during its redistribution and from isotope fractionation that may accompany the diffusive transport of gaseous Cd during migration in the parent bodies.

Rosman et al. (1980b) report a correlation between Cd isotope fractionation and Cd concentrations for chondrules, matrix separates and whole rock samples of the Tieschitz H/L 3.6 chondrite. They interpret the correlation as a mixing line between an unfractionated component and a component with a heavy Cd isotope composition that is associated with the chondrule separates. Rosman and De Laeter (1988) suggested that the two components resulted from a heterogeneous mix of precursor materials and/or from variable conditions in the solar nebula. For example, Cd isotope fractionation could have occurred during chondrule formation. However, chondrules are also present in the Allende and Murchison meteorites, but these meteorites do not display Cd isotope fractionations. Furthermore, chondrule formation is an unlikely cause for the heterogeneous distribution patterns that are associated with the Cd isotope fractionations in the ordinary chondrites. We suggest that the Tieschitz matrix contains some primary unfractionated Cd, whereas the component with the heavy Cd isotope composition recondensed in Tieschitz following volatilization and migration of Cd due to thermal metamorphism of the parent body. While both Cd components are present in the Tieschitz matrix, the initially Cd-poor chondrules may preferentially reflect the vapor-derived heavy Cd component.

Overall, we favor the explanation that open system thermal metamorphism on parent bodies generated the Cd isotope fractionations observed in the ordinary and Rumuruti chondrites.

4. SUMMARY AND CONCLUSIONS

A new technique that uses MC-ICPMS for the accurate and precise determination of the stable isotope composition of Cd in geological materials and meteorites is presented. External reproducibilities of ± 1.1 εCd/amu were achieved on a routine basis with $\sim$20 ng of Cd per analysis. Precise and accurate data, however, can be obtained with as little as 5 ng of Cd.

Cadmium data acquired with mass bias correction methods that involve external normalization to admixed Ag have reproducibilities that are superior to results obtained with the standard-sample bracketing method. However, after rejection of a few outliers, reasonably precise (± 2 εCd/amu) and accurate data were also produced with the standard-sample bracketing method.

With the exception of a layered tektite, analyses of terrestrial rocks and minerals displayed only a limited variability of ~ 2 εCd/amu in Cd isotope compositions. First evidence for small terrestrial Cd isotope fractionation is provided by the results obtained from sedimentary rocks. Furthermore, detectable isotope fractionations resulted from the sequential elution of Cd from anion-exchange resin and during coprecipitation of Cd with aragonite in the laboratory. The data for the aragonite sample, minerals that formed during weathering, and the sedimentary rocks suggests that natural (inorganic?) low-temperature processes will not result in substantial ($\gg 2$ εCd/amu) Cd isotope fractionations.

Large Cd isotope fractionations were identified for a layered tektite and some chondritic meteorites. Both sample types were thermally processed during their formation. The lack of substantial Cd isotope fractionation during natural (inorganic) processes together with the large fractionation observed for the chondritic meteorites and the tektite sample suggests that significant Cd isotope fractionations are generated only by partial evaporation and condensation. Therefore, the application of Cd stable isotopes is most promising for the identification of evaporation and condensation processes in cosmochemistry, impact-related studies, and investigations of volcanic and anthropogenic emissions of Cd into the environment.

The lack of resolvable Cd isotope fractionations between the primitive CI-chondrite Orgueil and the volatile element depleted CM- and CV-type carbonaceous chondrites and the silicate Earth is consistent with previous results for K isotopes (Humayun and Clayton, 1995). Both the Cd and the K data imply that the volatile element depletion of the inner solar system was not generated by Rayleigh evaporation. In contrast to K isotopes, the absence of Cd isotope fractionations in the carbonaceous chondrites and the Earth can be explained by a two-component mixture (Larimer and Anders, 1967; Wolf et al., 1980) of a refractory and a volatile element-rich component. If accretion or giant impacts led to a further depletion of Cd in the Earth, these processes did not involve extensive Rayleigh evaporation.

The Cd isotope fractionation observed for ordinary and Rumuruti chondrites is thought to result from the volatilization, migration and recondensation of Cd during open system thermal metamorphism of the parent bodies. Therefore, the calculation of accretion temperatures from the abundances of highly volatile elements is probably meaningless. Ultimately, further investigations will be required to address this question. Studies of the Cd distribution within meteorite samples would be particularly helpful in this regard.

Acknowledgments—This study was supported by a grant from the Deutsche Forschungsgemeinschaft to K.M. The paper benefited from insightful reviews by Jean-Marc Luck and Aaron Pietruszka and from additional comments by Jane Barling. Addi Bischoff (Institut für Planetologie, Münster), Monica Grady (Natural History Museum, London), Glenn MacPherson (Smithsonian Institution, Washington, DC) and

Jutta Zipfel (Max Planck Institut, Mainz) are thanked for providing meteorite samples. We are grateful to Alex Deutsch (Münster), Martin Dietzel (Graz), Hartmut Heinrichs and Günter Schnorrer (Göttingen) for providing rock and mineral samples and to Christoph Altmiks from Vacuum Technology in Aalen for the VTA-3 Cd metal. Simon Meffan-Main is thanked for additional data for VTA-3 Cd. Heidi Bayer, Michael Feldhaus and Dieter Garbe-Schönberg (Kiel) provided valuable technical support. FW thanks Alex Halliday for generous access to the ETH Zürich Nu Plasma lab.

Associate editor: R. Walker

REFERENCES

Anbar A. D., Knab K. A., and Barling J. (2001) Precise determination of mass-dependent variations in the isotopic composition of molybdenum. *Anal. Chem.* **73,** 1425–1431.

Anders E., Higuchi H., Ganapathy R., and Morgan J. W. (1976) Chemical fractionations in meteorites—IX. C3 chondrites. *Geochim. Cosmochim. Acta* **40,** 1131–1139.

Anders E. and Grevesse N. (1989) Abundances of the elements: Meteoritic and solar. *Geochim. Cosmochim. Acta* **53,** 197–214.

Belshaw N. S., Freedman P. A., O'Nions R. K., Frank M., and Guo Y. (1998) A new variable dispersion double-focusing plasma mass spectrometer with performance illustrated for Pb isotopes. *Int. J. Mass Spectrom.* **181,** 51–58.

Carlson R. W. and Hauri E. H. (2001) Extending the ^{107}Pd-^{107}Ag chronometer to low Pd/Ag meteorites with multicollector plasma-ionization mass spectrometry. *Geochim. Cosmochim. Acta* **65,** 1839–1848.

Chizhikov D. M. (1966) *Cadmium.* Pergamon Press.

Dietzel M. and Usdowski E. (1996) Coprecipitation of Ni^{2+}, Co^{2+}, and Mn^{2+} with galena and covellite, and of Sr^{2+} with calcite during crystallization via diffusion of H_2S and CO_2 through polyethylene at 20°C: Power law and Nernst law control of trace element partitioning. *Chem. Geol.* **131,** 55–65.

Dodd R. T. (1969) Metamorphism of the ordinary chondrites: A review. *Geochim. Cosmochim. Acta* **33,** 161–203.

Esat T. M. (1988) Physicochemical isotope anomalies. *Geochim. Cosmochim. Acta* **52,** 1409–1424.

Esat T. M. (1996) Comment on "Potassium isotope cosmochemistry: Genetic implications of volatile element depletion" by Munir Humayun and R. N. Clayton. *Geochim. Cosmochim. Acta* **60,** 3755–3758.

Gao X. and Thiemens M. H. (1993) Variations of the isotopic composition of sulfur in enstatite and ordinary chondrites. *Geochim. Cosmochim. Acta* **57,** 3171–3176.

Gussone N., Eisenhauer A., Heuser A., Dietzel M., Bock B., Böhm F., Spero H. J., Lea D. W., Bijma J., Zeebe R., and Nägler T. F. (2003) Model for kinetic effects on calcium isotope fractionation (δ^{44}Ca) in inorganic aragonite and cultured planktonic foraminifera. *Geochim. Cosmochim. Acta* **67,** 1375–1382.

Heinrichs H., Schulz-Dobrick B., and Wedepohl K. H. (1980) Terrestrial geochemistry of Cd, Bi, Tl, Pb, Zn and Rb. *Geochim. Cosmochim. Acta* **44,** 1519–1533.

Hirata T. (1997) Isotopic variations of germanium in iron and stony iron meteorites. *Geochim. Cosmochim. Acta* **61,** 4439–4448.

Humayun M., Clayton R. N., and Koeberl C. (1994) Potassium isotopic composition of some Australasian tektites. *Lunar Planet. Sci. Conf.* **25,** 581–582.

Humayun M. and Clayton R. N. (1995) Potassium isotope cosmochemistry: Genetic implications of volatile element depletion. *Geochim. Cosmochim. Acta* **59,** 2131–2148.

Keays R. R., Ganapathy R., and Anders E. (1971) Chemical fractionations in meteorites-IV. Abundances of fourteen trace elements in L-chondrites; implications for cosmothermometry. *Geochim. Cosmochim. Acta* **35,** 337–363.

Kettrup B., Deutsch A., Masaitis V. L. (2003) Homogeneous impact melts produced by a heterogeneous target? Sr-Nd isotopic evidence from the Popigai crater, Russia. *Geochim. Cosmochim. Acta* **67,** 733–750.

Koeberl C. (1992) Geochemistry and origin of Muong Nong-type tektites. *Geochim. Cosmochim. Acta* **56,** 1033–1064.

Larimer J. W. (1973) Chemical fractionations in meteorites-VIII. Cosmothermometry and cosmobarometry. *Geochim. Cosmochim. Acta* **37,** 1603–1623.

Larimer J. W. and Anders E. (1967) Chemical fractionations in meteorites-II. Abundance patterns and their interpretation. *Geochim. Cosmochim. Acta* **31,** 1239–1270.

Laul J. C., Ganapathy R., Anders E., and Morgan J. W. (1973) Chemical fractionations in meteorites-VI. Accretion temperatures of H-, LL-, and E-chondrites, from abundance of volatile trace elements. *Geochim. Cosmochim. Acta* **37,** 329–357.

Lee D.-C. and Halliday A. N. (1995) Precise determination of the isotopic compositions and atomic weights of molybdenum, tellurium, tin and tungsten using ICP magnetic sector multiple collector mass spectrometry. *Int. J. Mass Spectrom. Ion Processes* **146/147,** 35–46.

Lipschutz M. E. and Woolum D. S. (1988) Highly labile elements. In *Meteorites and the Early Solar System* (eds. J. F. Kerridge and M. S. Matthews), pp. 463–487. University of Arizona Press.

Longerich H. P., Fryer B. J., and Strong D. F. (1987) Determination of lead isotope ratios by inductively coupled plasma-mass spectrometry (ICP-MS). *Spectrochim. Acta* **42B,** 39–48.

Loss D. L., Rosman K. J. R., and De Laeter J. R. (1984) Mass spectrometric isotope dilution analysis of palladium, silver, cadmium and tellurium in carbonaceous chondrites. *Geochim. Cosmochim. Acta* **48,** 1677–1681.

Loss R. D., Rosman K. J. R., and De Laeter J. R. (1990) The isotopic composition of zinc, palladium, silver, cadmium, tin, and tellurium in acid-etched residues of the Allende Meteorite. *Geochim. Cosmochim. Acta* **54,** 3525–3536.

Luck J. M., Ben Othman D., Barret J. A., and Albarède F. (2001) Cu and Zn isotopic variations in meteorites. *Lunar Planet. Sci. Conf.* **32,** 1688.

Luck J. M., Ben Othman D., and Albarède F. (2002) What do Cu-Zn isotopes tell us on meteorites? (abstract). *Geochim. Cosmochim. Acta* **66,** A462.

Maréchal C. N., Télouk P., and Albarède F. (1999) Precise analysis of copper and zinc isotopic compositions by plasma-source mass spectrometry. *Chem. Geol.* **156,** 251–273.

Masaitis V. L. and Deutsch A. (1999) Popigai: Gneiss bombs coated with impact melt—Heating in the fireball? *Lunar Planet. Sci. Conf.* **30,** 1237.

McDonough W. F. (1999) Earth's core. In *Encyclopedia of Geochemistry* (eds. C. Marshall and R. Fairbridge), p. 712. Kluwer Academic.

Morgan J. W., Janssens M.-J., Takahashi H., Hertogen J., and Anders E. (1985) H-chondrites: Trace element clues to their origin. *Geochim. Cosmochim. Acta* **49,** 247–259.

Münker C., Weyer S., Scherer E., and Mezger K. (2001) Separation of high field strength elements (Nb, Ta, Zr, Hf) and Lu from rock samples for MC-ICPMS measurements. *Geochem. Geophys. Geosyst.* **2,** 2001.GC000183.

Nagahara H. and Ozawa K. (2000) Isotopic fractionation as a probe of heating processes in the solar nebula. *Geochim. Cosmochim. Acta* **169,** 45–68.

Ozawa K. and Nagahara H. (2001) Chemical and isotopic fractionations by evaporation and their cosmochemical implications. *Geochim. Cosmochim. Acta* **65,** 2171–2.

Palme H. (2001) Chemical and isotopic heterogeneity in protosolar matter. *Phil. Trans. R. Soc. Lond. A* **359,** 1–15.

Palme H., Larimer J. W., and Lipschutz M. E. (1988) Moderately volatile elements. In *Meteorites and the Early Solar System* (eds. J. F. Kerridge and M. S. Matthews), pp. 436–461. University of Arizona Press.

Rehkämper M. and Halliday A. N. (1999) The precise measurement of Tl isotopic compositions by MC-ICPMS: Application to the analysis of geological materials and meteorites. *Geochim. Cosmochim. Acta* **63,** 935–944.

Rehkämper M. and Mezger K. (2000) Investigation of matrix effects for Pb isotope ratio measurements by multiple collector ICP-MS: Verification and application of optimized analytical protocols. *J. Anal. At. Spectrom.* **15,** 1451–1460.

Rehkämper M., Schönbächler M., and Stirling C. H. (2001) Multiple collector ICP-MS: Introduction to instrumentation, measurement techniques and analytical capabilities. *Geostand. Newsl.* **25,** 23–40.

Rehkämper M., Wombacher F., and Aggarwal J. K. (in press) Stable isotope analysis by multiple collector ICP-MS. In *Handbook of Stable Isotope Analytical Techniques* (ed. P. D. Groot). Elsevier.

Rosman K. J. R. and De Laeter J. R. (1974) The abundance of cadmium and zinc in meteorites. *Geochim. Cosmochim. Acta* **38,** 1665–1677.

Rosman K. J. R. and De Laeter J. R. (1975) The isotopic composition of cadmium in terrestrial materials. *Int. J. Mass Spectrom. Ion Proc.* **16,** 385–394.

Rosman K. J. R. and De Laeter J. R. (1976) Isotopic fractionation in meteoritic cadmium. *Nature* **261,** 216–218.

Rosman K. J. R. and De Laeter J. R. (1978) A survey of cadmium isotopic abundances. *J. Geophys. Res.* **83,** *B3*, 1279–1287.

Rosman K. J. R., Barnes I. L., Moore L. J., and Gramlich J. W. (1980a) Isotope composition of Cd, Ca and Mg in the Brownfield chondrite. *Geochem. J.* **14,** 269–277.

Rosman K. J. R., De Laeter J. R., and Gorton M. P. (1980b) Cadmium isotope fractionation in fractions of two H3 chondrites. *Earth Planet. Sci. Lett.* **48,** 166–170.

Rosman K. J. R. and De Laeter J. R. (1988) Cadmium mass fractionation in unequilibrated ordinary chondrites. *Earth Planet. Sci. Lett.* **89,** 163–169.

Rubin A. E., Scott E. R. D., Taylor G. J., and Keil K. (1984) The Dimmitt H chondrite regolith breccia and implications for the structure of the H chondrite parent body (abstract). *Meteoritics* **16,** 382–383.

Russel W. A., Papanastassiou D. A., and Tombrello T. A. (1978) Ca isotope fractionation on the Earth and other solar system materials. *Geochim. Cosmochim. Acta* **42,** 1075–1090.

Sands D. G., Rosman K. J. R., and de Laeter J. R. (2001) A preliminary study of cadmium mass fractionation in lunar soils. *Earth Planet. Sci. Lett.* **186,** 103–111.

Siebert C., Nägler T. F., and Kramers J. D. (2001) Determination of molybdenum isotope fractionation by double-spike multicollector inductively coupled plasma mass spectrometry. *Geochem. Geophys. Geosyst.* **2,** 2000.GC000124.

Stöffler D., Keil K., and Scott E. R. D. (1991) Shock metamorphism of ordinary chondrites. *Geochim. Cosmochim. Acta* **55,** 3845–3867.

Strelow F. W. E. (1978) Improved separation of cadmium from indium, zinc, gallium and other elements by anion-exchange chromatography in hydrobromic-nitric acid mixtures. *Anal. Chim. Acta* **100,** 577–588.

Thirlwall M. (2001) Inappropriate tail corrections can cause large inaccuracy in isotope ratio determination by MC-ICP-MS. *J. Anal. At. Spectrom.* **16,** 1121–1125.

Tomascak P. B., Carlson R. W., and Shirey S. B. (1999) Accurate and precise determination of Li isotopic compositions by multi-collector sector ICP-MS. *Chem. Geol.* **158,** 145–154.

Vance D. and Thirlwall M. (2002) An assessment of mass discrimination in MC-ICPMS using Nd isotopes. *Chem. Geol.* **185,** 227–240.

Wai C. M. and Wasson J. T. (1977) Nebular condensation of moderately volatile elements and their abundances in ordinary chondrites. *Earth Planet. Sci. Lett.* **36,** 1–13.

Walder A. J. and Furuta N. (1993) High-precision lead isotope ratio measurement by inductively coupled plasma multiple collector mass spectrometry. *Anal. Sci.* **9,** 675–680.

Wang J., Davis A. M., Clayton R. N., and Hashimoto A. (1999) Evaporation of single crystal forsterite: Evaporation kinetics, magnesium isotope fractionation, and implications of mass-dependent isotopic fractionation of a diffusion controlled reservoir. *Geochim. Cosmochim. Acta* **63,** 953–966.

Wasson J. T. (1991) Layered tektites: A multiple impact origin for the Australasian tektites. *Earth Planet. Sci. Lett.* **102,** 95–109.

White W. M., Albarède F., and Télouk P. (2000) High-precision analysis of Pb isotope ratios by multi-collector ICP-MS. *Chem. Geol.* **167,** 257–270.

Wolf R., Richter G. R., Woodrow A. B., and Anders E. (1980) Chemical fractionations in meteorites-XI. C2 chondrites. *Geochim. Cosmochim. Acta* **44,** 711–717.

Wolf S. F. and Lipschutz M. E. (1998) Chemical studies of H chondrites 9: Volatile trace element composition and petrographic classification of equilibrated H chondrites. *Meteorit. Planet. Sci.* **33,** 303–312.

Yi W., Halliday A.-N., Lee D.-C., and Christensen J.-N. (1995) Indium and tin in basalts, sulfides, and the mantle. *Geochim. Cosmochim. Acta* **59,** 5081–5090.

Yi W., Halliday A. N., Lee D.-C., and Rehkämper M. (1998) Precise determination of cadmium, indium and tellurium using multiple collector ICP-MS. *Geostand. Newsl.* **22,** 173–179.

Young E. D. (2000) Assessing the implications of K isotope cosmochemistry for evaporation in the preplanetary solar nebula. *Earth Planet. Sci. Lett.* **183,** 321–333.

Young E. D., Nagahara H., Mysen B. O., and Audet D. M. (1998) Non-Rayleigh oxygen isotope fractionation by mineral evaporation: Theory and experiments in the system SiO_2. *Geochim. Cosmochim. Acta* **62,** 3109–3116.